

# Evaluation of the Performance of Thermal Diffusion Columns Separating Xenon Isotopes

SAMUEL BLUMKIN and EDWARD VON HALLE

Union Carbide Nuclear Company, Oak Ridge, Tennessee

Three thermal diffusion columns of the hot-wire type have been employed in a laboratory to test their effectiveness in the separation of the isotopes of xenon. The laboratory data have been analyzed by a procedure to be described and the experimentally derived values for the column separation parameters have been compared with those predicted by theory. The results establish an empirical basis for the design of a thermal diffusion plant for the separation of xenon isotopes.

## DESCRIPTION OF THE EXPERIMENTS

### Equipment and Operating Conditions

Each of the three experimental hot-wire columns at the laboratory has an I.D. of  $\frac{3}{4}$  in. and an effective height of 24 ft. The wire is  $\frac{1}{16}$ -in. thick and is centered by spacers at 4-ft. intervals. The ratio of the column radius to the wire radius is thus 12.0. The columns have no reservoirs at either end.

The hot-wire operating temperature is given as  $900^{\circ}\text{C}$ . The columns are water-cooled and the average cold-wall temperature is assumed to be  $20^{\circ}\text{C}$ . The ratio of hot to cold temperature is thus 4.0.

The columns were filled in the cold state with feed gas to pressures ranging from 25 to 150 mm. mercury. This corresponds to a range of 83 to 249 mm. mercury at the operating temperature. The feed gas was not naturally occurring xenon but a mixture of four isotopes of atomic weights 131, 132, 134, and 136.

### Experimental Results

Both steady and unsteady state separation data, under total reflux operating conditions, were collected by the laboratory investigators. The data consist of the Xenon-131 and Xenon-136 content of samples taken simultaneously from the top and bottom of a column, the time elapsed between startup and sample drawoff, and the gas pressure in the column at start-up. Samples were reported at various times from 1 to 12 hr. for the transient condition experiments, and all samples for the equilibrium runs were taken at 17 hr. after start-up. Equilibrium runs at five or more different pressures were made with each column. The transient experiments, however, consisted only of a single run with each column, but at a different pressure in each.

## ANALYSIS OF DATA

### The Transport Equation

The net transport of a component of a binary mixture separating in a thermal diffusion column, with no product withdrawal, is given by

$$\tau = Hx(1-x) - (K_c + K_d) \frac{dx}{dz} \quad (1)$$

where  $H$ ,  $K_c$ , and  $K_d$  are the thermal diffusion transport coefficients reflecting the separating efficiency of the column.

The transport coefficient,  $H$ , involves the thermal diffusion effect to which the separation is proportional. The other coefficients,  $K_c$  and  $K_d$ , represent remixing effects which are opposed to the thermal diffusion separating effect.

The net transport equation is basic for making plant design calculations. For the design of a thermal diffusion cascade, the transport coefficients,  $H$  and  $K_c + K_d$  must be known. Most often, one has no choice but to evaluate them theoretically. When these column parameters can be determined from test data, one's confidence in the adequacy of a resulting design is increased considerably.

### Definition of the Column Transport Coefficients

The thermal diffusion column transport coefficients are functions of the column dimensions and geometry, the operating conditions, and certain properties of the process gas. Jones and Furry (1), in their well-known classic exposition of thermal diffusion theory and its application to column design, have formulated these coefficients for several geometries. The expressions for the coefficients for the extreme cylindrical case, that is the hot wire type of column, are

$$H = \frac{2\pi g}{6!} \left( \frac{\alpha \rho^2}{\eta} \right)_1 r_1^4 \cdot h \left( \frac{T_2}{T_1}, \frac{r_1}{r_2} \right) \quad (2)$$

$$K_c = \frac{2\pi g^2}{9!} \left( \frac{\rho^3}{\eta^2 D} \right)_1 r_1^8 \cdot k_c \left( \frac{T_2}{T_1}, \frac{r_1}{r_2} \right) \quad (3)$$

and

$$K_d = 2\pi (\rho D)_1 r_1^2 \cdot k_d \left( \frac{T_2}{T_1}, \frac{r_1}{r_2} \right) \quad (4)$$

where  $\alpha$  is the thermal diffusion constant defined, for a binary mixture, by

$$\alpha = \frac{105}{118} \left( \frac{M_2 - M_1}{M_2 + M_1} \right) (kT^*)_1 \quad (5)$$

The subscript 1 associated with the temperature-dependent gas properties indicates that values for these to be used in computing the transport coefficients are at the cold-wall temperature. It is seen from these equations that the thermal diffusion effect as represented by the thermal diffusion constant,  $\alpha$ , appears only in the expression for  $H$ . Equations (2), (3), and (4) are simplified forms of more complex expressions involving certain integrals which are represented here by the symbols  $h$ ,  $k_c$ , and  $k_d$  and are generally referred to as shape factors. With the assumption of the Maxwellian model for gases, Jones and Furry have evaluated the shape factor integrals numerically.

Recently, McInTeer and Reisfeld (2) and Greene and Von Halle (3) have extended the work of Jones and Furry to include non-Maxwellian as well as Maxwellian gases and also to cover a considerably wider range in column geometry and operating temperatures.

McInTeer and Reisfeld assumed the Lennard-Jones 6-12 potential model in their evaluation, thereby introducing the Lennard-Jones reduced temperature as an additional argument in their tabulation of shape factors. A specific relation between  $\alpha$  and temperature, determined for each gas by the values of its force constants, is implied by the model. Jones and Furry had assumed  $\alpha$  to be independent of temperature.

In their treatment, Greene and Von Halle adopted the inverse power repulsion law to represent the gas molecular interaction. Some basic relationships involved in this model are the assumption

$$F \propto \frac{1}{d^{\nu}}$$

Then

$$\nu = \frac{2n + 3}{2n - 1}$$

and  $\eta/T^n$ ,  $\lambda/T^n$ ,  $\rho D/T^n$ , and  $D/T^{n+1}$  are independent of temperature.

A Maxwellian gas is a particular instance of this model, since for it  $n = 1$ . Greene and Von Halle have computed the shape factors for  $n = 0.5, 0.6, 0.7, 0.8, 0.9$ , and  $1.0$ . They recognized that for most gases the thermal diffusion constant increases with temperature and have evaluated and tabulated the shape factor,  $h$ , for three cases:  $\alpha$  independent of temperature,  $\alpha$  proportional to  $T^{1/2}$ , and  $\alpha$  proportional to  $T$ .

For some gases, and xenon is one of them, the variation of  $\alpha$  with temperature is not at all well represented by a simple function of  $T^{1/2}$  or  $T$ , but is more closely fitted by a polynomial, such as

$$\alpha = A_0 + A_{1/2} T^{1/2} + A_1 T \quad (6)$$

where  $A_0$ ,  $A_{1/2}$ , and  $A_1$  are constants. The use of this relation leads to modified expression for the transport coefficient,  $H$

$$H = \frac{2\pi g}{6!} \left( \frac{\rho^2}{\eta} \right)_1 r_1^4 \cdot h^* \left( \frac{T_2}{T_1}, \frac{r_1}{r_2} \right) \quad (7)$$

where

$$h^* = A_0 h_0 + A_{1/2} h_{1/2} T_1^{1/2} + A_1 h_1 T \quad (8)$$

and where  $h_0$ ,  $h_{1/2}$ , and  $h_1$  are the appropriate Greene and Von Halle tabulated values of  $h$  for  $\alpha$  proportional to  $T^0$ ,  $T^{1/2}$ , and  $T^1$ , respectively.

#### Transport Coefficients from Separation Data

**Equilibrium Data.** Integration of the differential net transport equation over the length of a column leads to

$$\ln \frac{\left( \frac{x}{1-x} \right)_T}{\left( \frac{x}{1-x} \right)_B} = \frac{Hz}{K_c + K_d} \quad (9)$$

where subscripts  $T$  and  $B$  refer to the top and bottom of the column, respectively. The ratio in the left-hand member of this equation is customarily called the column separation factor and is denoted by the symbol,  $q$ , that is

$$q \equiv \frac{\left( \frac{x}{1-x} \right)_T}{\left( \frac{x}{1-x} \right)_B}$$

Now, it is evident that the transport coefficients  $H$  and  $K_c$  are pressure dependent. If these are expressed simply in terms of the column operating pressure by

$$H = H' p^2$$

$$K_c = K_c' p^4$$

then Equation (9) can be rewritten to give

$$\ln q = \frac{(H'/K_c') \frac{z}{p^2}}{1 + \frac{(K_d/K_c')}{p^4}} \quad (10)$$

With equilibrium separation data obtained at several different operating pressures, one can then correlate the  $q$  values with the pressures, applying the above function, to obtain the ratios  $H'/K_c'$  and  $K_d/K_c'$ . Values of the individual coefficients are indeterminate from such data alone.

It can be demonstrated simply that  $q$  is a maximum when  $K_d/K_c' = p^4$ ; that is, when  $K_d = K_c$ . It should be pointed out that the pressure at which the isotopic enrichment is a maximum is not the optimum operating pressure, since it is not the pressure at which the column will produce the maximum separative work.

**Unsteady State Data in Combination with Equilibrium Data.** The transport coefficients may be determined individually by analysis of the transient separation data in conjunction with equilibrium data at the same operating pressure. This is accomplished by the use of the equation given below which expresses the time dependency of the concentration at the top of a separating column. This equation, because of assumptions made in its derivation, is applicable only for a short initial period after start-up, for a narrow enrichment span, and for a column without a reservoir at either end. The concentration at the top of the column as a function of time is given by

$$\frac{y_T}{y_0} = 1 + \frac{4\theta^{1/2}}{\pi^{1/2}} + 2\theta + \dots \quad (11)$$

where

$$y_T = ax_T + b$$

$$y_0 = ax_0 + b$$

$$\theta = \frac{H^2 z}{4(K_c + K_d)} \cdot \frac{a^2 t}{I}$$

and  $a$  and  $b$  are constants used to linearize the quadratic term,  $x(1-x)$ , appearing in the basic differential transport equation.

The usefulness of this relationship lies in the fact that for sufficiently small values of  $\theta$  (short time after start-up),  $y_T/y_0$  is linear with respect to  $\theta^{1/2}$ . If the slope of a straight line drawn through the early time data on a plot of  $y_T/y_0$  vs.  $\sqrt{t}$  is denoted by  $m$ , then

$$m = 4 \left( \frac{\theta'}{\pi} \right)^{1/2} \quad (12)$$

where  $\theta'$  is defined by  $\theta \equiv \theta' t$ .

If Equation (12) is solved for  $\theta'$

$$\theta' = \frac{\pi m^2}{16} \quad (13)$$

But  $\theta'$  is expressible in terms of the transport coefficients and can be related to the equilibrium data for the same column under the same operating conditions by

$$\frac{\theta'}{\ln q} = \frac{a^2 H}{4I} \quad (14)$$

so that  $H$  can be expressed in terms of the measured value of the slope as

$$H = \frac{\pi I m^2}{4a^2 \ln q} \quad (15)$$

By means of Equation (15) it is therefore possible to obtain an experimental value for the transport coefficient,  $H$ , from the slope of the initial linear portion of the line representing  $y_T/y_0$  vs.  $\sqrt{t}$  and a measured value of the overall separation factor,  $q$ , at equilibrium. Further, since  $H'/K_c'$  and  $K_d/K_c'$  can be found from the correlation of the equilibrium data with the operating pressures,  $K_c'$  and  $K_d$  can also be individually evaluated.

The unsteady state data obtained from the bottom of the column can be employed in similar fashion. The time dependency of the bottom concentration is given by

$$y_B/y_0 = 1 - \frac{4\theta^{1/2}}{\pi^{1/2}} + 2\theta \text{-----} \quad (16)$$

Equation (15) applies without modification to the bottom transient data.

### Separative Work

A measure which is very useful in comparing the efficiency of complex separation plants or the units comprising them is a quantity called separative work,  $U$ , which for a thermal diffusion column is written

$$U = \frac{H^2 z}{4(K_c + K_d)} \quad (17)$$

If the total separative work required to produce a given product concentration at a given rate is determined from cascade productivity calculations, and the separative work produced by a column is known, then the number of such columns required for the job is a matter of simple arithmetic.

### Multicomponent System

No consideration has been made in the above discussion of the fact that the data to be analyzed involve a multicomponent mixture rather than a binary one.

With regard to equilibrium data, the multicomponent case is uncomplicated. In a multicomponent system the ratio of the concentrations of any pair of components at the top and bottom of a column at steady state, operating with no product withdrawal, is independent of the concentrations of the other components present. Thus for the case considered in this study, the column separation factor for the Xenon-131 and Xenon-136 pair,  $q_1$ , is defined simply by

$$q_1 = \frac{(x_1/x_6)_T}{(x_1/x_6)_B}$$

where subscripts 1 and 6 refer to Xenon-131 and Xenon-136, respectively, and subscripts  $T$  and  $B$  refer, as before, to the top and bottom of the column, respectively.

In terms of the transport coefficients, then

$$\ln q_1 = \frac{H_1 z}{K_c + K_d} = \frac{(H_1'/K_c') \frac{z}{p^2}}{1 + \frac{(K_d/K_c')}{p^4}} \quad (18)$$

where the thermal diffusion constant incorporated in  $H_1$  is defined as

$$\alpha_1 = \frac{105}{118} \cdot \frac{M_6 - M_1}{M_6 + M_1} k_T^* \quad (19)$$

With regard to the transient data the presence of additional components must be taken into account. The unsteady state equations given above are based on the relation for the net transport of a component in a binary mixture. For a multicomponent system the net transport equation is more complex as shown by the following expression for the transport of one component in a four-component mixture (4):

$$\tau_1 = H_1 x_1 (1 - x_1) - H_2 x_1 x_2 - H_3 x_1 x_3 - (K_c + K_d) \frac{dx_1}{dz} \quad (20)$$

The subscripts 1, 2, and 3 refer to each of three components.

Instead of attempting the extremely difficult and laborious task involved in developing the transient equations directly from Equation (20), one can make an approximation that circumvents the problem. This is accomplished with a definition of an average diffusive transport coefficient,  $\bar{H}$ , as follows:

$$\bar{H} = H_1 - \frac{H_2 x_2}{1 - x_1} - \frac{H_3 x_3}{1 - x_1} \quad (21)$$

Equation (20) can then be rewritten in the binary form of the transport equation

$$\tau_1 = \bar{H} x_1 (1 - x_1) - (K_c + K_d) \frac{dx_1}{dz} \quad (22)$$

Since  $H_2$  and  $H_3$  can be written in terms of  $H_1$ , Equation (21) can be reduced to a simple proportionality between  $\bar{H}$  and  $H_1$ , which for the xenon mixture under consideration becomes

$$\bar{H} = \omega H_1$$

where  $\omega$  is a constant.

This permits the expression of the unsteady state equations for the multicomponent mixture in terms of  $H_1$  rather than  $\bar{H}$ . The redefinition of the variable  $\theta$  in the transient equation is then

$$\theta = \frac{\omega^2 H_1^2 z}{K_c + K_d} \cdot \frac{a^2 t}{4I}$$

Equation (15) then becomes

$$H_1 = \frac{\pi I m^2}{4\omega^2 a^2 \ln q_1} \quad (23)$$

The separative work for this multicomponent system is arbitrarily defined in terms of  $H_1$  so that Equation (17) becomes

$$U = \frac{H_1^2 z}{4(K_c + K_d)} \quad (24)$$

## CORRELATIONS AND RESULTS

### Theoretical

The required properties of xenon, such as the viscosity, the coefficient of ordinary diffusion, and the thermal diffusion constant were computed at several temperatures by means of the equations based on the Lennard-Jones 6-12 potential model (5). Three sets of the transport coefficients ( $H_1'$ ,  $K_c'$ , and  $K_d$ ) were then computed for the laboratory columns with the shape factors of Jones and Furry, McInteer and Reisfeld, and Greene and Von Halle. Since the ratio of column-to-wire radius of 12.0 was smaller than the lowest value of 15.0 tabulated by Jones and Furry, it was necessary to make a graphical extrapolation of their values.

To obtain Greene and Von Halle shape factors, estimates are necessary of the viscosity index,  $n$ , and a simi-

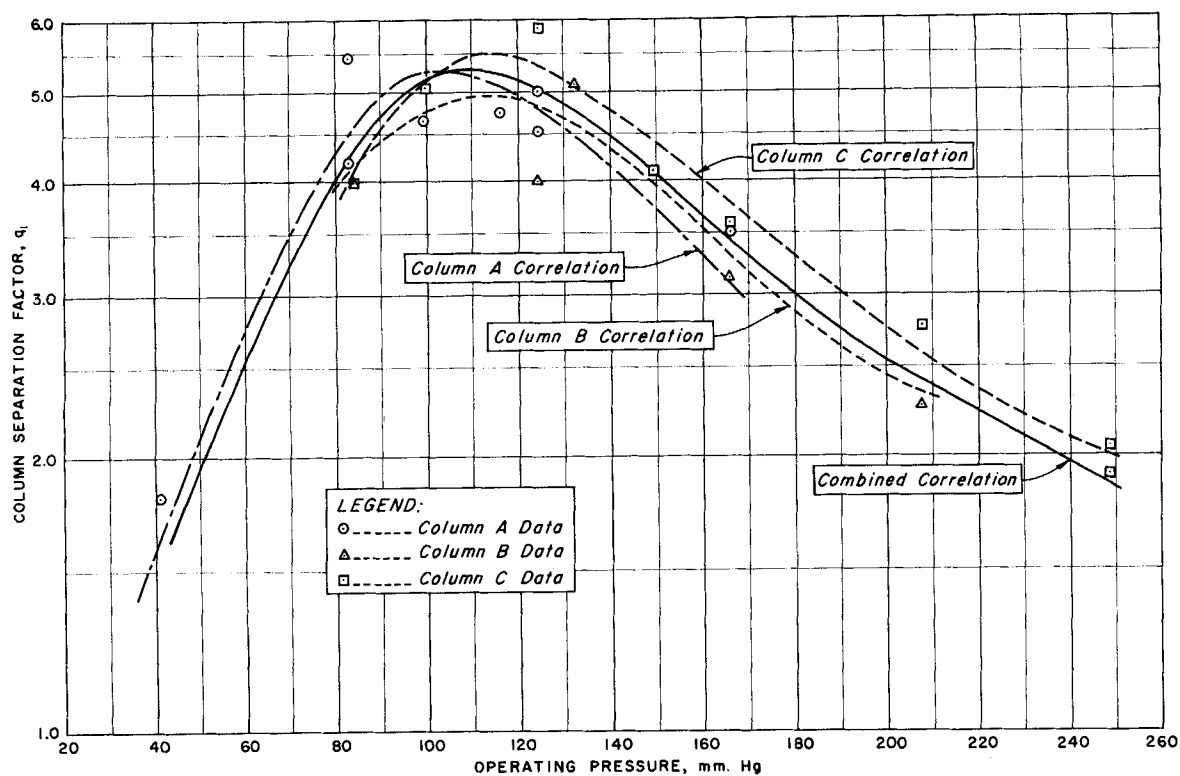


Fig. 1. Correlation of the observed column equilibrium separation factors with pressure.

lar one for the thermal diffusion constant. An average value of 0.81 for the viscosity index over the temperature range of interest, 293° to 1,172°K., represents the curve reasonably well. On the other hand the shape of the  $\alpha$  vs.  $T$  curve is such that a simple power function of temperature makes a very poor fit. However the polynomial as expressed in Equation (6) above results in a fit that is essentially congruent to the curve for almost the whole range of interest. Thus the following relationship for  $\alpha$  was used in conjunction with Equations (7) and (8) to obtain the Greene and Von Halle value of  $H_1$ :

$$\alpha = -0.01733 + 0.00145 T^{1/2} - 0.0000197 T \quad (25)$$

Entry into the McIner and Reisfeld tabulation requires a Lennard-Jones reduced temperature value, which for xenon at the cold-wall temperature of 20°C. is 1.28. The three sets of theoretically evaluated transport coefficients are given in Table 1. The Jones and Furry values differ from the other two sets to a significantly greater extent than the latter do from each other. This is not

surprising since the non-Maxwellian behavior of the xenon molecule and the variation of the thermal diffusion constant with temperature is at least approximated by the latter.

#### Experimental

**The Equilibrium Data.** The column separation factors,  $q_1$ , were computed from the equilibrium Xenon-131 and Xenon-136 concentrations. These  $q_1$  values were correlated by the method of least squares with the operating pressures with the application of Equation (18). The data and the correlations are presented in Figure 1. Four curves have been drawn, three of them representing separate correlations of the individual column data and the fourth giving the correlation of all the data combined into a single set. The data are somewhat scattered; the 95% confidence limits on the computed parameters (which represent  $H_1/K_c'$  and  $K_d/K_c'$  values) are  $\pm 7\%$  to  $\pm 20\%$  of the value of the parameters. Table 2 lists these parameters, the maximum  $q_1$  values, and the operating pressure at which  $q_1$  is a maximum for each column and also for an average column as determined from the correlation of all the data as a single set. It should be remembered that the values of the individual transport coefficients are not obtainable from just equilibrium enrichment and pressure data, but only the ratios:  $H_1/K_c'$  and  $K_d/K_c'$ .

From the three sets of theoretical transport coefficients given in Table 1 three theoretical  $q_1$  vs.  $p$  curves were computed and

TABLE 1. THEORETICAL AND EXPERIMENTAL VALUES OF THE COLUMN TRANSPORT COEFFICIENTS

	$H_1'$ , g. sec.-atm. <sup>2</sup>	$K_c'$ , g.-cm. sec.-atm. <sup>4</sup>	$K_d$ , g.-cm. sec.
Theoretical			
Jones and Furry shape factors	0.000147	2.63	0.00154
McIner and Reisfeld shape factors	0.000582	4.07	0.00137
Greene and Von Halle shape factors			
theoretical $\alpha$	0.000540	4.62	0.00132
experimental $\alpha$	0.000465		
Experimental			
From top concentration data	0.000632	6.69	0.00289
From bottom concentration data	0.000251	2.66	0.00115

TABLE 2. TRANSPORT COEFFICIENTS, MAXIMUM ENRICHMENT, AND PRESSURE FOR MAXIMUM ENRICHMENT FROM THE COLUMN EQUILIBRIUM DATA

	Column A	Column B	Column C	Average column
Transport coefficients				
( $H_1'/K_c'$ ) $\times 10^4$	0.8459	0.9374	1.057	0.9608
( $K_d/K_c'$ ) $\times 10^3$	0.3448	0.4343	0.5205	0.4403
Maximum enrichment, $q_1$	5.27	4.97	5.49	5.33
Operating (hot) pressure at which the enrichment is a maximum, mm. mercury	101	116	115	110

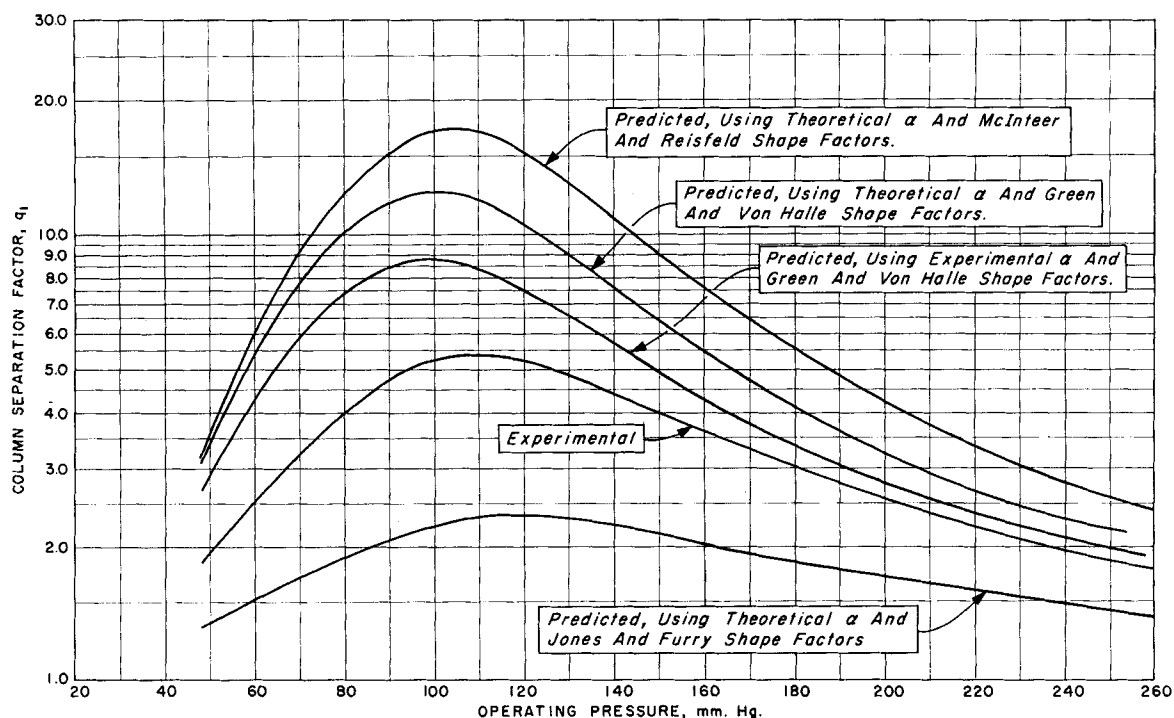


Fig. 2. Comparison of predicted column separation factors with the experimental values.

plotted in Figure 2 along with the curve from Figure 1 representing the correlation of the combined experimental data. It is evident from Figure 2 that the pressure at which the enrichment is a maximum is fairly well predicted by all three sets of theoretical values. This is not so with respect to the magnitude of the maximum separation: the McInteer and Reisfeld values overstate it by a factor of 3.2, the Greene and Von Halle values overstate it by a factor of 2.3, and the Jones and Furry values understate it by a factor of 2.3. It should be noted here that there is a considerable degree of uncertainty in the value of the shape factor,  $h$ , as obtained from the McInteer and Reisfeld tables by interpolation. In the region of interest the variation of  $h$  with the reduced temperature is markedly nonlinear, and the span of tabulated values is too large to interpolate with confidence in the accuracy of the result.

Moran and Watson (6) have reported measurements, made with a swing-separator apparatus, of the thermal diffusion factor for xenon in the range of 200° to 600°K. Their data were generally lower than the values predicted by the Lennard-Jones 6-12 model. This can be seen from Figure 3 where both the Lennard-Jones theoretical values and the Moran and Watson data are plotted. It is of interest then to incorporate the experimental  $\alpha$  values into a recomputation of the theoretical  $q_1$  vs.  $p$  curves. It is obvious that such a correction to the Jones and Furry curve would lead to a result having a still greater deviation from the experimental column data, and would therefore be pointless. Further, such a correction to the other two sets would leave their relative position with respect to each other unchanged. Logically, then, for the comparison being made, the correction need be applied only to the set which is closer to the column data, that is, to the Greene and Von Halle values.

An excellent polynomial fit to the Moran and Watson  $\alpha$  data was obtained and is given by

$$\alpha_M = -0.00873 + 0.000805 T^{1/2} - 0.00000950 T \quad (26)$$

When the coefficients in this relation were utilized, a revised value of  $H_1'$  was evaluated (see Table 1) which with the  $K_c'$  and  $K_d$  values previously computed, yielded a semiempirical  $\ln q_1$  vs.  $p$  curve, based on Greene and Von Halle shape factors and embodying the experimental thermal diffusion factors. This curve is also shown in Figure 2. The factor of 2.34 by which the maximum enrichment is overstated using the theoretical Lennard-Jones  $\alpha$  relationship is now reduced to a factor of 1.65.

The equilibrium time increases as the degree of enrichment is increased or the operating pressure is decreased, so that it is a

maximum at a pressure a bit lower than that which gives the maximum enrichment. Estimates made of the equilibrium times for xenon in these columns indicate that at operating pressures of 75 to 110 mm. mercury, the steady state concentrations had not yet been attained at 17 hr. after start-up, which time all equilibrium run samples are reported to have been taken. The indication is that at these pressures about 95 to 96% of the equilibrium Xenon-131 concentration had been attained. One must conclude then that some bias exists in the peak of the experimental  $\ln q_1$  vs.  $p$  curve in Figure 2. It is noteworthy that the deviation between the experimental curve and the closer of the Greene and Von Halle curves is significantly greater at the peak than it is at the ends of the curves.

**Correlation of the Transient Data with the Equilibrium Data.** The transient data for the three columns are plotted in Figures 4, 5, and 6 in the form of  $y_r/y_0$  and  $y_b/y_0$  values for Xenon-131 vs. the square root of time. Also plotted are the steady state values from the equilibrium run or runs made at the same pressure as the transient run in the particular column. For comparison, curves representing the concentration-time functions of Equations (11) and (16) are also shown. The values of  $H'$

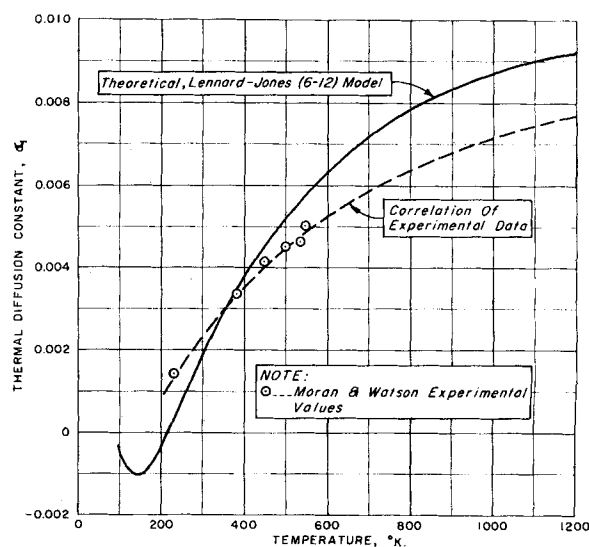


Fig. 3. Theoretical and experimental values of the thermal diffusion constant.

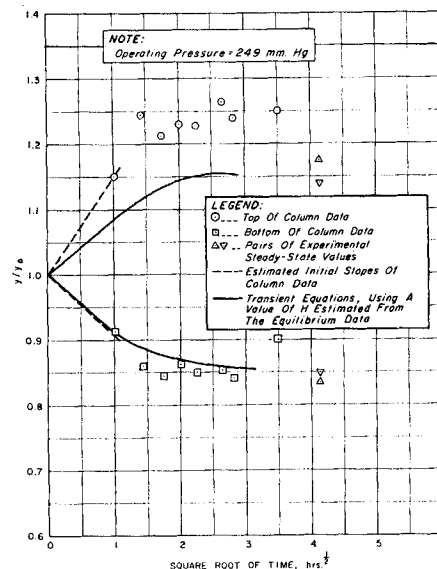
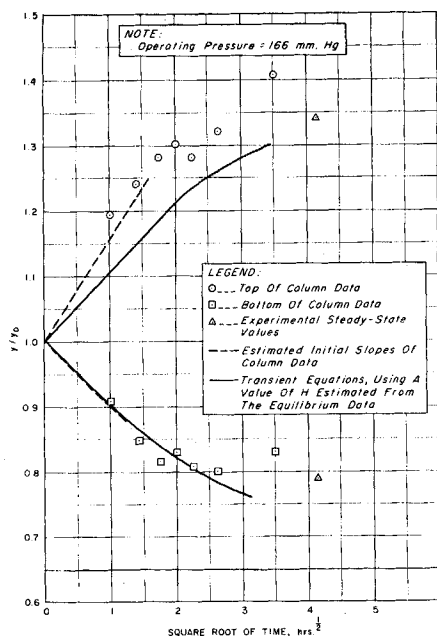
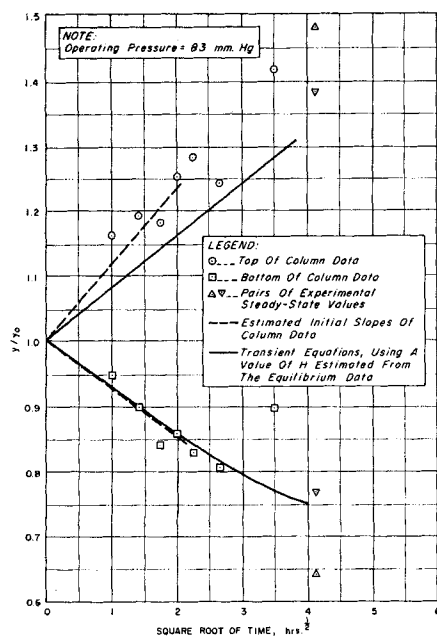


Fig. 4. Xenon-131 transient data from column A. Fig. 5. Xenon-131 transient data from column B. Fig. 6. Xenon-131 transient data from column C.

used to compute these curves were extracted from the steady state data by making the assumption that the deviation between the experimental and predicted  $H_1'/K_c'$  value for each column is owing entirely to error in the prediction of  $H_1'$ . Note that the curves representing the time dependence of the top concentration fall appreciably below the main body of corresponding data for each column, but the ones representing the bottom concentration pass through or lie very close to the experimental values. Furthermore the top transient data for columns B and C trend to higher concentrations than those of the corresponding equilibrium data. Inspection of the transient data and the matching equilibrium data points for column A indicates that steady state conditions had not been reached at 17 hr. The transient run in this column was made at a hot pressure of 83 mm. mercury (cold pressure, 50 mm. mercury). This tends to corroborate the contention already made regarding the probable existence of a bias in some of the steady state data.

Straight lines approximating the early time data are drawn in Figures 4, 5, and 6. The slopes of these lines were then used in equation (12) to compute an average experimental  $H_1$  value. With  $H_1'$  known, the other two transport coefficients were computed from the  $H_1'/K_c'$  and  $K_d/K_c'$  obtained from the steady state data. The results of this analysis of the top and bottom unsteady state data differ significantly and are given in Table 1. To explain this large discrepancy, one might speculate that the Xenon-131 concentration in the feed gas was actually slightly greater than that reported. If an initial Xenon-131 concentration were assumed such that the slopes of the lines representing early time bottom and top transient data are equal, a reestimation of the column transport coefficients should give results approximating averages of the values previously obtained from the two sets of data. Note that average values of the experimental transport coefficients given in Table 1 are in fairly close agreement with the semiempirical Greene and Von Halle values.

**Separative Work.** The separative work produced by a thermal diffusion column is a function of the operating pressure. Theoretically it is an ever increasing function approaching an upper limit asymptotically. In actual practice, however, the separative work passes through a maximum owing to the effect of turbulence at higher pressures. Jones and Furry indicate that the maximum performance occurs generally for operating conditions such that  $K_c/K_d$  is about equal to ten. Values for the separative work and operating pressures when  $K_c = 10 K_d$  were computed from both sets of experimentally derived transport coefficients and the sets of theoretical ones. These are given in Table 3. The separative work derived from the top transient data is greater by a factor of 2.5 than that obtained from analysis of the bottom transient data. Note here that the average of the two experi-

mental values is closest to the semiempirical Greene and Von Halle values. The  $K_c$  to  $K_d$  ratio is determinate from just the steady state data, so that the estimate of pressure at which this condition occurs is unaffected by any bias in the transient data.

## CONCLUSION

The two sets of unsteady state data, column top concentrations and column bottom concentrations, are inconsistent with each other in that they yield widely different values of the transport coefficients. A plausible explanation for this is to assume that the reported content of Xenon-131 in the feed gas is a bit low. If so, the actual performance of the thermal diffusion columns approximates the average of the two sets of results. Also, there is a small bias near the peak enrichment values for the equilibrium data, since there is evidence that some data were taken before steady state was reached.

With respect to the prediction of the transport coefficients, it was expected and has been found that the shape factors of Jones and Furry lead to results significantly different from the other two sets and also very probably furthest from the true values. This is in consequence

TABLE 3. THEORETICAL AND EXPERIMENTAL ESTIMATES OF MAXIMUM SEPARATIVE WORK

	Separative work, g./day	Operating pressure at which separative work is a maximum,* mm. mercury
Theoretical		
With Jones and Furry shape factors	0.118	210
With McInteer and Reisfeld shape factors	1.194	183
With Greene and Von Halle shape factors		
theoretical $\alpha$	0.906	176
experimental $\alpha$	0.672	176
Experimental		
From top transient data	0.872	195
From bottom transient data	0.346	195

\* The maximum is assumed to occur at the pressure which  $K_c = 10 K_d$ .

of the fact that xenon does not behave as a Maxwellian gas and its thermal diffusion constant is strongly temperature dependent.

The agreement of the McInteer and Reisfeld values with those of Greene and Von Halle is fair. In the opinion of the authors, the differences in the theoretical values obtained with these two bases stem primarily from the evident uncertainty of the interpolation in the McInteer and Reisfeld tables, and only secondarily from the consequences of the differences in the model representing the molecular interaction. It is expected that estimates using McInteer and Reisfeld shape factors would be, in general, similar to those using Greene and Von Halle values.

In predicting the actual performance of the columns the most successful basis is the one utilizing the Greene and Von Halle shape factors in conjunction with a correlation of experimental values of the thermal diffusion factor for xenon. The fact that this basis gives significantly better agreement with experiment than the McInteer and Reisfeld basis is owing largely to the use of an empirical thermal diffusion factor-temperature dependence instead of the theoretical Lennard-Jones (6 to 12) relationship. It is in the feasibility of incorporating such experimental information that the use of the set of shape factors computed by Greene and Von Halle is particularly advantageous.

#### ACKNOWLEDGMENT

The authors thank G. R. Grove and his colleagues at the Mound Laboratory at Miamisburg, Ohio, for making their data available for this analysis and for their courtesy and cooperation in discussions in this regard.

#### NOTATION

$A_0, A_{1/2}, A_1$  = constants in the  $\alpha$  vs.  $T$  relation given in Equation (6)  
 $a$  = one of the two constants used to linearize the quadratic term  $x(1-x)$  in the transport equation for the time dependent solution:  $x(1-x) = ax + b \equiv y$   
 $b$  = a constant (see definition of  $a$ )  
 $D$  = the coefficient of ordinary diffusion of the process gas  
 $d$  = the distance between molecules  
 $F$  = the force of repulsion between molecules  
 $g$  = the acceleration of gravity  
 $H$  = a column transport coefficient, see Equations (2) and (8)  
 $H_1$  = the value of  $H$  for  $\alpha = \alpha_1$   
 $H'$  =  $H/p^2$   
 $\bar{H}$  = an average  $H$  value in a multicomponent system defined by Equation (21)  
 $h$  = a shape factor, see Equation (2)  
 $h_0$  = the Greene and Von Halle value of  $h$  for  $\alpha$  proportional to  $T^0$   
 $h_{1/2}$  = the Greene and Von Halle value of  $h$  for  $\alpha$  proportional to  $T^{1/2}$   
 $h_1$  = the Greene and Von Halle value of  $h$  for  $\alpha$  proportional to  $T^1$   
 $h^*$  = the value of  $h$  defined by Equation (7)  
 $I$  = the column inventory  
 $K_c$  = a column transport coefficient, see Equation (3)  
 $K_c'$  =  $K_c/p^4$   
 $K_d$  = a column transport coefficient, see Equation (4)  
 $k_c$  = a shape factor, see Equation (3)  
 $k_d$  = a shape factor, see Equation (4)  
 $kt^*$  = the ratio of the thermal diffusion ratio as predicted from the Lennard-Jones 6-12 model to the value based on the rigid sphere model

$M_1, M_2$  = the atomic or molecular weights of the isotopic species of the process gas  
 $m$  = the slope of the early time  $y/y_0$  values vs.  $t^{1/2}$   
 $n$  = the viscosity index  
 $p$  = the operating (hot) column pressure  
 $q$  = the column separation factor for the binary case  
 $q_1$  = the column separation factor in the multicomponent case defined specifically here in terms of the Xenon-131 and Xenon-136 concentrations  
 $r_1, r_2$  = the radii of the outer and inner annular surfaces of the column, respectively  
 $T$  = the absolute temperature  
 $T_1, T_2$  = the absolute temperatures of the cold and hot annular surfaces in the column respectively  
 $t$  = time  
 $U$  = the separative work, see Equations (17) and (24)  
 $x$  = the concentration of the desired component  
 $x_B$  =  $x$  at the column bottom  
 $x_0$  =  $x$  at  $t = 0$   
 $x_T$  =  $x$  at the column top  
 $z$  =  $ax + b$ ;  $y_B = ax_B + b$ ; etc.  
 $y$  = the effective column height

#### Greek Letters

$\alpha$  = the thermal diffusion constant or factor defined by Equation (5), reflects the Lennard-Jones (6-12)  $k_T^*$  values  
 $\alpha_1$  = the value of  $\alpha$  specifically defined for the separation of Xenon-131 from Xenon-136, see Equation (19)  
 $\alpha_M$  = the value of the thermal diffusion factor from a correlation of the Moran and Watson xenon experimental data  
 $\eta$  = the viscosity of the process gas  
 $\theta$  = a variable in the time-dependent concentration equation, see Equation (11)  
 $\theta'$  =  $\theta/t$   
 $\lambda$  = the thermal conductivity of the process gas  
 $\nu$  = the force index  
 $\rho$  = the density of the process gas  
 $\tau$  = the net transport of the desired component in a binary system  
 $\tau_1$  = the net transport of the desired component in a multicomponent system  
 $\omega$  = a constant dependent upon the components and their concentrations in the feed mixture

#### LITERATURE CITED

1. Jones, R. C., and W. H. Furry, *Rev. Mod. Phys.*, **18**, 151-224 (1946).
2. McInteer, B. B., and M. J. Reisfeld, "Tabulated Values of the Thermal Diffusion Column Shape Factors for the Lennard-Jones (12-6) Potential," LAMS-2517, Los Alamos Scientific Laboratory, Los Alamos, New Mexico (February, 1961).  
 McInteer, B. B., and M. J. Reisfeld, *J. Chem. Phys.*, **33**, 570-8 (1960).
3. Greene, E., and Edward Von Halle, "Calculation of the Shape Factors for Thermal Diffusion Columns Based on the Inverse Power Law," Union Carbide Nuclear Company, Oak Ridge, Tennessee (K-1469, to be published).
4. Von Halle, Edward, "Multicomponent Fractionation," (AECU-3902), Union Carbide Nuclear Company, Oak Ridge, Tennessee (August, 1956).
5. Hirshfelder, J. O., C. F. Curtiss, and R. B. Bird, "Molecular Theory of Gases and Liquids," pp. 552-84, Wiley, New York (1954).
6. Moran, T. I., and W. W. Watson, *Phys. Rev.*, **109**, 1184-90 (1958).

Manuscript received November 7, 1962; revision received March 1, 1963; paper accepted March 5, 1963. Paper presented at A.I.Ch.E. Denver meeting.